

Preparation, Structure, and Electronic Properties of a Low-Spin Iron(II) Hexaamine Compound

Heidi Börzel, Peter Comba,* Hans Pritzkow, and Achim F. Sickmüller

Anorganisch-Chemisches Institut der Universität, Im Neuenheimer Feld 270,
D-69120 Heidelberg, Germany

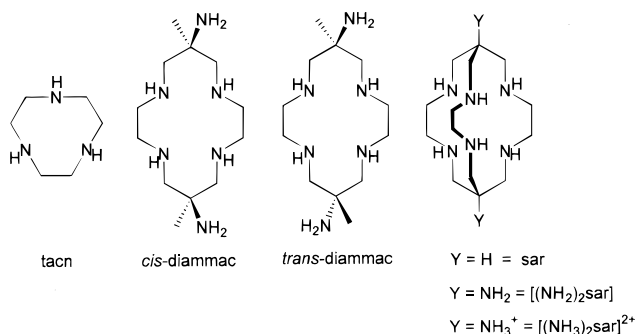
Received December 10, 1997

[Fe(*trans*-diammac)]²⁺ (*trans*-diammac = *exo*-6,13-diamino-6,13-dimethyl-1,4,8,11-tetraazatetradecane) is one of the very few fully characterized examples of a low-spin iron(II) compound with saturated amine ligands. The crystal structure analysis (monoclinic, *P*2₁/*c*; *a* = 9.547(8), *b* = 14.631(13), *c* = 16.91(2) Å; β = 98.92(7)°; *Z* = 4) defines the iron(II) coordination geometry as distorted octahedral with very short in-plane Fe–N distances (average of 2.01 Å) to the secondary amines of the macrocyclic ligand and slightly longer distances to the pendant primary amine donors (2.03 Å); there is a considerable tilt of the vector involving the axial donors with respect to the plane defined by the secondary amines and the metal center (θ = 11.5°). The metal–donor distances are shorter than those for other low-spin iron(II) hexaamines, and consequently, the redox potential (Fe^{3+/2+}) is very small (0.45 V vs SHE) and the ligand field splitting is very large (*Dq* = 1785 cm⁻¹). The structural, magnetic, and spectroscopic properties are discussed on the basis of the experimental data in comparison with model studies.

Introduction

The nitrogen donor coordination chemistry of low-spin iron(II) is dominated by aromatic amines such as bipy (2,2'-bipyridine) and phen (1,10-phenanthroline) which are strong σ donors and weak π acceptors. Due to the lower ligand field exerted by aliphatic amines, there are only very few examples of hexaamine iron(II) coordination compounds with low-spin electronic configuration. Thus, their spectroscopic and structural properties are still relatively unexplored. So far, there are only two relevant examples that have been studied in detail: (i) The iron(II) compounds of the sar-type hexaamine cage ligands (sar = 3,6,10,13,16,19-hexaazabicyclo[6.6.6]eicosane; (NH₂)₂sar = 1,8-diamino-3,6,10,13,16,19-hexaazabicyclo[6.6.6]eicosane, [(NH₃)₂sar]²⁺ = 1,8-diammonio-3,6,10,13,16,19-hexaazabicyclo[6.6.6]eicosane; Chart 1) are, depending on the specific ligand and the environment (solid or solution), close to the high-spin/low-spin crossover, and no experimental structural data for these compounds with low-spin electronic configuration have been reported.¹ (ii) [Fe(tacn)₂]X₂·4H₂O (X = Cl⁻, Br⁻; tacn = 1,4,7-triazacyclononane; Chart 1) has a low-spin electronic configuration, and detailed structural, magnetic, and spectroscopic properties have been reported (removal of the water yields a paramagnetic material with a temperature-dependent magnetic moment).² For both, the cage and the bis-tacn compounds, detailed studies of the corresponding low-spin iron(III) (d⁵) and the cobalt(III) (low-spin d⁶) complexes are also available.^{1–4}

Chart 1



The bis-pendant amine tetraazamacrocyclic hexaamine ligand diammac (diammac = 6,13-diamino-6,13-dimethyl-1,4,8,11-tetraazatetradecane) exists in two isomeric forms, with the pendant primary amines *exo* or *endo* with respect to the macrocyclic ligand plane (*cis*- and *trans*-diammac, respectively; Chart 1). While *cis*-diammac leads to relatively long metal–amine bond distances, those of *trans*-diammac are extremely short. Coordination compounds of *trans*-diammac exist in three conformations (Chart 2), and the relative stability of these depends on the metal ion preference in terms of the metal–donor bond distance. The *δδ* isomer is the most stable form for metal–donor distances slightly larger than 2 Å, and this is the expectation for low-spin iron(II). Detailed structural and spectroscopic studies have been reported for low-spin [Fe(*trans*-diammac)]³⁺ (d⁵)⁷ and for [Co(*trans*-diammac)]³⁺ (d⁶).⁸

We report the synthesis and the electronic and structural properties of low-spin [Fe(*trans*-diammac)]²⁺. These are analyzed on the basis of model calculations (MM and MM-

(1) (a) Martin, L. L.; Martin, R. L.; Sargeson, A. M. *Polyhedron* **1994**, *13*, 1969. (b) Martin, L. L.; Martin, R. L.; Murray, K. S.; Sargeson, A. M. *Inorg. Chem.* **1990**, *29*, 1387.

(2) (a) Wiegardt, K.; Schmidt, W.; Herrmann, W.; Küppers, H. J. *Inorg. Chem.* **1983**, *22*, 2953. (b) Wiegardt, K.; Küppers, H. J.; Weiss, J. *Inorg. Chem.* **1985**, *24*, 3067. (c) Boeyens, J. C. A.; Forbes, A. G. S.; Hancock, R. D.; Wiegardt, K. *Inorg. Chem.* **1985**, *24*, 2926.

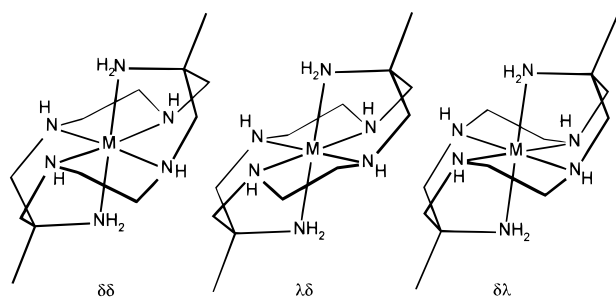
(3) (a) Geue, R. J.; Hambley, T. W.; Harrowfield, J. M.; Sargeson, A. M.; Snow, M. R. *J. Am. Chem. Soc.* **1984**, *106*, 5478. (b) Comba, P.; Sargeson, A. M.; Engelhardt, L. M.; Harrowfield, J. M.; White, A. H.; Horn, E.; Snow, M. R. *Inorg. Chem.* **1985**, *24*, 2325.

(4) Koyama, H.; Yoshino, T. *Bull. Chem. Soc. Jpn.* **1972**, *45*, 481.

(5) Bernhardt, P. V.; Comba, P. *Helv. Chim. Acta* **1991**, *74*, 1834; **1992**, *75*, 645.

(6) Comba, P.; Hambley, T. W. *Molecular Modeling of Inorganic Compounds*; VCH: Weinheim, Germany, 1995.

Chart 2



AOM for the structures and ligand field spectra, respectively) and compared with those of other low-spin hexaamine iron(II) compounds and with those of the cobalt(III) and the low-spin iron(III) compounds of *trans*-diammac.

Experimental Section

Syntheses. The preparation of *trans*-diammac·6HCl has been described previously.^{8,9} Neutralization of the hydrochloride salt by anion exchange chromatography (Amberlite IRA 400) yielded the free base *trans*-diammac as a colorless powder in 94% yield. Mp: 127 °C. ¹H NMR (200 MHz, D₂O, δ (ppm) vs internal TSP): 0.8 (s, 6H, CH₃); 2.34, 2.26 (AB, dd, 8H, CH₂, propylene bridge); 2.42 (s, 8H, CH₂, ethylene bridge). ¹³C NMR (50.54 MHz, D₂O, δ (ppm) vs internal MeOH at 50.2 ppm): 24.74 (CH₃), 46.91 (CH₂, ethylene bridge), 50.68 (quaternary C), 57.86 (CH₂, propylene bridge).

Samples of iron(II) compounds were handled under nitrogen (Schlenk techniques) and in rigorously deoxygenated solvents. An aqueous solution (2 mL) of FeSO₄·7 H₂O (253 mg, 0.91 mmol) was transferred by syringe to an aqueous solution (2 mL) of the ligand (250 mg, 0.91 mmol). The deep blue solution of the product was stirred at room temperature for 30 min. Addition of an aqueous solution (2 mL) of NH₄PF₆ (321 mg, 1.82 mmol) produced a blue precipitate which was collected on a filter, washed with water and then EtOH (twice) and Et₂O before drying in vacuo (150 mg, 0.25 mmol, 27%). ¹H NMR (200 MHz, D₂O, δ): 0.99 (s, CH₃); 2.19 (d, CH₂, propylene bridge); 2.62 (d, CH₂, ethylene bridge); 3.03 (d, CH₂, propylene bridge); 3.16 (d, CH₂, ethylene bridge). Anal. Calcd for C₁₂F₁₂FeH₃₀N₆P₂: C, 23.85; H, 4.97; N, 13.91. Found: C, 23.65; H, 5.01; N, 13.99. Pure, dry [Fe(*trans*-diammac)]²⁺ is stable over months when kept under nitrogen. Blue crystals, suitable for X-ray analysis, were isolated from a saturated aqueous solution at 5 °C.

Spectroscopy. Electronic spectra were recorded on a Perkin-Elmer λ19 UV-vis-NIR spectrometer. For NMR spectroscopy a Bruker EM200 instrument was used (D₂O, references, TSP, MeOH). IR spectra (KBr disks) were measured on a Perkin-Elmer 1650 FT-IR spectrometer. Magnetic moments were determined by the Faraday technique, and diamagnetic corrections were made using Pascals constants. Elemental analyses were performed by the Microanalytical Section of the Chemical Institutes at Heidelberg, Germany.

Structure Determination. Reflexes of a representative crystal were measured at 203(2) K. Intensity measurements data were obtained from a Siemens STOE-AED2 diffractometer, using MoKα-radiation and operating in the ω-scan mode. The structure was solved by direct methods (SHELXS 86^{10a}) and refined by full matrix least-squares methods based on F² (SHELXL 93^{10b}), using anisotropic thermal

Table 1. Crystallographic Data for [Fe(diammac)](PF₆)₂

| | |
|---|---|
| chem formula | C ₁₂ H ₃₀ F ₁₂ FeN ₆ P ₂ ·H ₂ O |
| M _r | 622.23 |
| T (K) | 203(2) |
| λ (Å) | 0.710 70 (Mo Kα) |
| space group | P2 ₁ /c |
| a (Å) | 9.547(8) |
| b (Å) | 14.631(13) |
| c (Å) | 16.91(2) |
| α (deg) | 90 |
| β (deg) | 98.92(7) |
| γ (deg) | 90 |
| V (Å ³) | 2333(4) |
| Z | 4 |
| ρ _{calc} (g cm ⁻³) | 1.771 |
| μ (mm ⁻¹) | 0.898 |
| R1 [I > 2 σ(I)] ^a | 0.0413 |
| wR2 (all data) ^b | 0.1088 |

$$^a R1 = [\sum ||F_o| - |F_c||] / \sum |F_o|. \quad ^b wR2 = [(\sum w(F_o^2 - F_c^2)^2) / (\sum w(F_o^2)^2)]^{1/2}.$$

Table 2. Selected Bond Distances (Å) and Valence Angles (deg) for [Fe(diammac)](PF₆)₂

| | | | |
|------------------|------------|-----------------|----------|
| Fe(1)–N(2) | 2.002(3) | N(2)–C(3) | 1.492(4) |
| Fe(1)–N(1) | 2.008(3) | N(2)–C(4) | 1.500(4) |
| Fe(1)–N(3) | 2.009(3) | N(3)–C(6) | 1.488(4) |
| Fe(1)–N(4) | 2.009(3) | N(3)–C(5) | 1.497(4) |
| Fe(1)–N(5) | 2.029(3) | N(4)–C(9) | 1.490(4) |
| Fe(1)–N(6) | 2.031(3) | N(4)–C(8) | 1.490(4) |
| N(1)–C(1) | 1.487(4) | N(5)–C(2) | 1.493(4) |
| N(1)–C(10) | 1.491(4) | N(6)–C(7) | 1.491(4) |
| N(2)–Fe(1)–N(1) | 93.30(12) | C(6)–N(3)–C(5) | 113.2(2) |
| N(2)–Fe(1)–N(3) | 87.56(12) | C(6)–N(3)–Fe(1) | 107.5(2) |
| N(1)–Fe(1)–N(3) | 177.60(9) | C(9)–N(4)–C(8) | 115(2) |
| N(2)–Fe(1)–N(4) | 177.89(9) | C(9)–N(4)–Fe(1) | 115.4(2) |
| N(1)–Fe(1)–N(4) | 86.36(12) | C(8)–N(4)–Fe(1) | 108.2(2) |
| N(3)–Fe(1)–N(4) | 92.86(12) | C(2)–N(5)–Fe(1) | 99.6(2) |
| N(2)–Fe(1)–N(5) | 80.66(11) | C(7)–N(6)–Fe(1) | 99.5(2) |
| N(1)–Fe(1)–N(5) | 83.52(12) | N(1)–C(1)–C(2) | 109.5(2) |
| N(3)–Fe(1)–N(5) | 98.82(11) | N(5)–C(2)–C(11) | 113.4(3) |
| N(4)–Fe(1)–N(5) | 97.23(11) | N(5)–C(2)–C(1) | 103.1(2) |
| N(2)–Fe(1)–N(6) | 98.19(11) | N(5)–C(2)–C(3) | 106.6(2) |
| N(1)–Fe(1)–N(6) | 97.11(12) | N(2)–C(3)–C(2) | 110.8(2) |
| N(3)–Fe(1)–N(6) | 80.55(11) | N(2)–C(4)–C(5) | 109.3(2) |
| N(4)–Fe(1)–N(6) | 83.92(11) | N(3)–C(5)–C(4) | 110.2(2) |
| N(5)–Fe(1)–N(6) | 178.72(10) | N(3)–C(6)–C(7) | 111.2(2) |
| C(1)–N(1)–C(10) | 115.2(2) | N(6)–C(7)–C(8) | 103.9(2) |
| C(1)–N(1)–Fe(1) | 108.3(2) | N(6)–C(7)–C(12) | 113.4(2) |
| C(10)–N(1)–Fe(1) | 108.2(2) | N(6)–C(7)–C(6) | 106.1(2) |
| C(3)–N(2)–C(4) | 112.9(2) | N(4)–C(8)–C(7) | 109.5(2) |
| C(3)–N(2)–Fe(1) | 107.7(2) | N(4)–C(9)–C(10) | 109.0(2) |
| C(4)–N(2)–Fe(1) | 107.1(2) | | |

parameters for all non-hydrogen atoms. All hydrogen atoms were located in a difference Fourier map and refined isotropically. The structure refined to wR2 = 0.108. Crystallographic data, selected bond distances and valence angles are given in Tables 1 and 2, respectively, and the ORTEP¹¹ diagram of Figure 1 shows the structure of the molecular cation with the atomic labeling scheme.

Calculations. The MOME97 program¹² and force field¹³ were used for force field calculations. Parameters not published before involve interactions between low-spin iron(II) (FE2L), high-spin iron(II) (FE2H), aliphatic amine (NT), and sp²-nitrogen in aromatic six-membered rings (NP). The parameters were fitted to low-spin [Fe(2-

- (7) (a) Bernhardt, P. V.; Lawrance, G. A.; Hambley, T. W. *J. Chem. Soc., Chem. Commun.* **1989**, 553. (b) Bernhardt, P. V.; Comba, P.; Lawrance, G. A.; Hambley, T. W. *Inorg. Chem.* **1991**, *30*, 842. (c) Stratemeier, H.; Hitchman, M. A.; Comba, P.; Bernhardt, P. V.; Riley, M. J. *Inorg. Chem.* **1991**, *30*, 4088. (d) Comba, P. *Inorg. Chem.* **1994**, *33*, 4577.
- (8) Bernhardt, P. V.; Lawrance, G. A.; Hambley, T. W. *J. Chem. Soc., Dalton Trans.* **1989**, 1059.
- (9) Comba, P.; Curtis, N. F.; Lawrance, G. A.; Sargeson, A. M.; Skelton, B. W.; White, A. H. *Inorg. Chem.* **1986**, *25*, 4260.
- (10) (a) Sheldrick, G. M. SHELXS 86, University of Göttingen, 1986. (b) Sheldrick, G. M. SHELXL 93, University of Göttingen, 1993.

- (11) Johnson, C. K. *ORTEP, A Thermal Ellipsoid Plotting Program*; Oak Ridge National Laboratory: Oak Ridge, TN, 1965.
- (12) Comba, P.; Hambley, T. W.; Lauer, G.; Okon, N. *MOME97, a Molecular Mechanics Program for Inorganic Compounds*; Lauer & Okon: Heidelberg, Germany, 1997 (e-mail: CVS-HD@T-Online.de).
- (13) (a) Bernhardt, P. V.; Comba, P. *Inorg. Chem.* **1992**, *31*, 2638. (b) Comba, P.; Hambley, T. W.; Ströhle, M. *Helv. Chim. Acta* **1995**, *78*, 2042. (c) Bol, J. E.; Buning, C.; Comba, P.; Reedijk, J.; Ströhle, M. *J. Comput. Chem.* **1998**, *19*, 512.

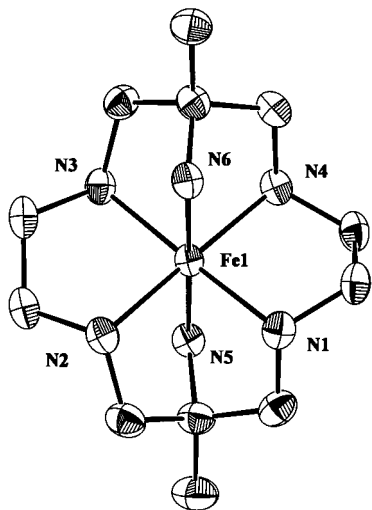


Figure 1. ORTEP drawing of $[\text{Fe}(\text{trans-diammac})]^{2+}$, showing the crystallographic numbering and the thermal vibrational (50%) ellipsoids.

$\text{pic})_3]^{14}$ (2-pic = 2-(methylamine)pyridine), high-spin $[\text{Fe}(\text{2-pic})_3]^{14}$ and $[\text{Fe}(\text{NH}_3)_2\text{sar}](\text{NO}_3)_2 \cdot \text{H}_2\text{O}$.¹ The angle bending around the donor atom was, as usual, assumed to be metal ion independent.¹³ Angle bending around the metal center was modeled with 1,3-nonbonded interactions alone.¹³ Bonding interaction [k (mdyn \AA^{-1}), r_0 (\AA): Fe2H–NT, 1.0, 2.200; FE2H–NP, 1.05, 2.195; FE2L–NT, 1.2, 2.0; FE2L–NP, 1.250, 1.995. CAMMAG^{7c,15} was used for the AOM calculations of the low-spin iron(II) compounds. The Condon–Shortley ($F_2 = 1112 \text{ cm}^{-1}$; $F_4 = 90 \text{ cm}^{-1}$) and ligand field parameters ($C(\text{RNH}_2) = 460\,000 \text{ cm}^{-1} \text{\AA}^6$; $C(\text{R}_2\text{NH}) = 470\,000 \text{ cm}^{-1} \text{\AA}^6$; $e_\sigma(r) = C/r^6$; $r = \text{Fe–N}$; i.e., for Fe–N = 2.0 \AA , $e_\sigma(\text{primary amine}) = 7188 \text{ cm}^{-1}$, and $e_\sigma(\text{secondary amine}) = 7344 \text{ cm}^{-1}$) were fitted to the electronic spectra of $[\text{Fe}(\text{NH}_2)_2\text{-sar}](\text{CF}_3\text{SO}_3)_2$,¹ $[\text{Fe}(\text{NH}_3)_2\text{sar}](\text{NO}_3)_2 \cdot \text{H}_2\text{O}$,¹ $[\text{Fe}(\text{tacn})_2]\text{Br}_2 \cdot 3\text{H}_2\text{O}$,² and $[\text{Fe}(\text{diammac})](\text{PF}_6)_2 \cdot \text{H}_2\text{O}$.

Results and Discussion

Reaction of iron(II) sulfate with *trans*-diammac in aqueous solution produces $[\text{Fe}(\text{trans-diammac})]^{2+}$ in moderate yield. In solution, the compound is very air-sensitive; the intense pink color of the decay product ($\lambda_{\text{max}} = 500 \text{ nm}$) indicates that the initial oxidation process might be followed by amine deprotonation. As a solid, $[\text{Fe}(\text{trans-diammac})](\text{PF}_6)_2$ is moderately stable when handled in an oxygen-free atmosphere. The air-sensitivity is a result of the low reduction potential ($E^\circ = 0.45 \text{ V vs SHE}$), and this was expected from the ligand's preference for small metal–donor distances and the high stability of $[\text{Fe}(\text{trans-diammac})]^{3+}$.^{5–7}

The low-spin electronic configuration of $[\text{Fe}(\text{trans-diammac})]^{2+}$ was expected from the ligand's preference for short metal–donor bond distances, and the experimentally determined structure, the observed NMR, and the electronic spectra are in good agreement with these expectations (see below). Variable-temperature magnetic susceptibility measurements (89–280 K) of $[\text{Fe}(\text{trans-diammac})](\text{PF}_6)_2$ (solid) showed no deviation from the room-temperature magnetic moment values, in agreement with the absence of a transition to the high-spin state. Low-spin iron(II) usually gives a temperature-independent susceptibility of approximately $50 \times 10^{-6} \text{ cgsu}$ ($\mu_{\text{eff}} \sim 0.6 \mu_{\text{B}}$), due to the second-order Zeemann interaction with higher ligand field terms.¹⁶ The value for $[\text{Fe}(\text{trans-diammac})](\text{PF}_6)_2$ ($\mu_{\text{eff}} = 1.20$

μ_{B}) is surprisingly high for spin-paired iron(II) compounds. The rather large residual moment might be due to the severe angular distortion (tilt angle $\theta = 11.5^\circ$; see section on structure below). However, the anomalous moment might also be due to some paramagnetic impurities because of the instability of the compound. It has been shown elsewhere that traces of less than 3% iron(III) can lead to a significant increase in the measured magnetic moment (up to more than $1 \mu_{\text{B}}$),¹⁷ and this would be difficult to detect in the electronic spectra.

The ¹H NMR spectrum of $[\text{Fe}(\text{trans-diammac})]^{2+}$ is very similar to that of $[\text{Zn}(\text{trans-diammac})]^{2+}$ and slightly different from that of $[\text{Co}(\text{trans-diammac})]^{3+}$, and all three are different from the spectrum of the metal-free ligand (signals for the zinc(II) and the cobalt(III) compounds and of the metal free ligand in parentheses): two doublets for the axial and the equatorial protons of the six-membered chelate rings, 2.19, 3.03 ppm (Zn^{II}, 2.50, 3.2 ppm; Co^{III}, 2.6, 3.4 ppm; ligand, 2.26, 2.34 ppm); an AB pattern for the axial and equatorial protons of the two methylene groups of the five-membered chelate rings, 2.62, 3.16 ppm (Zn^{II}, 2.6, 3.3; Co^{III}, 2.9, 3.6; ligand (singlet), 2.42); a low-field singlet for the terminal methyl group at 0.99 ppm (Zn^{II}, 1.19 ppm; Co^{III}, 1.35 ppm; ligand, 0.8 ppm). The spectroscopic similarity may indicate common structural features of the coordination compounds, and this was investigated by an analysis of the solid-state structure of $[\text{Fe}(\text{trans-diammac})]^{2+}$ and by molecular mechanics calculations. Note that the observed structures of the zinc(II) and cobalt(III) compounds (solid state) have different conformations ($\delta\delta$ and $\lambda\delta$, respectively; see Chart 2), and the predicted conformations in solution, based on molecular mechanics, are identical to those observed in the solid state.^{5,6}

The molecular structure of $[\text{Fe}(\text{trans-diammac})]^{2+}$ is shown in Figure 1, and selected geometric parameters are assembled in Table 2. The pendant arm macrocycle is coordinated as a hexadentate ligand, with the two primary amines (N(5) and N(6)) in axial positions trans to each other ($178.72(10)^\circ$). The angle θ between the axis through N(5), the metal center, and N(6) and the best plane involving the remaining donors and the metal center is 11.48° . δ conformations for the two five-membered chelate rings are evident from the crystallographically analyzed structure. This isomer has been predicted to be the most stable for metal ions with metal–amine bond distances in the range of approximately 1.98 \AA to approximately 2.25 \AA (note that the hole size analysis depends on the method used to vary the bond distances^{5,6,18}). The observed bond distances (Fe–N = 2.007, 2.03 \AA) are in good agreement with these predictions, and they are slightly shorter than those for the other well-characterized low-spin iron(II) compounds ($[\text{Fe}(\text{tacn})_2]\text{Cl}_2 \cdot \text{H}_2\text{O}$, Fe–N = 2.035 \AA).²

Table 3 reports the pertinent structural features for the $[\text{Fe}(\text{trans-diammac})]^{2+}$ molecular cation in comparison with those of the corresponding zinc(II), cobalt(III), and iron(III) compounds. For all four structures the equatorial metal–donor distances are considerably shorter than the bonds to the axial ligands. The bonds to cobalt(III) are the shortest in this series, and indeed, these are the shortest cobalt(III)–amine bonds reported for aliphatic amine donors so far. The difference in bond distances between the cobalt(III) and the low-spin iron(III) and that between the cobalt(III) and the low-spin iron(II)

(14) Sinn, E. *J. Am. Chem. Soc.* **1978**, *100*, 8080.

(15) Gerloch, M. *Cammag*, a Fortran Program for AOM calculations; University of Cambridge: Cambridge, U.K., 1991.

(16) Figgis, B. N. *Introduction to Ligand Fields*; Interscience: New York, N. Y., **1966**, 280.

(17) Sinn, E. *Inorg. Chim. Acta* **1969**, *3*, 11.

(18) (a) Comba, P. *Coord. Chem. Rev.* **1993**, *123*, 1. (b) Comba, P. In *Molecular modeling and dynamics of bioinorganic compounds*; Banci, L., Comba, P., Eds.; Kluwer Academic Publishers: Dordrecht, Boston, London, 1997; p 21.

Table 3. Observed and Calculated Structural Parameters of Transition Metal Complexes of *trans*-diammac

| structural params | Fe(III) $\delta\delta$ | Co(III) $\lambda\delta$ | Zn(II) $\delta\delta$ | Fe(II) $\delta\delta$ |
|-----------------------|------------------------|-------------------------|-----------------------|-----------------------|
| M–N _{ax} (Å) | | | | |
| X-ray | 1.984 | 1.946 | 2.210 | 2.030 |
| MM | 1.984 | 1.945 | 2.200 | 2.030 |
| M–N _{eq} (Å) | | | | |
| X-ray | 1.976 | 1.937 | 2.10 | 2.007 |
| MM | 1.982 | 1.936 | 2.106 | 2.019 |
| θ (deg) | | | | |
| X-ray | 10.5 | 9.00 | 14.75 | 11.48 |
| MM | 9.2 | 2.7 | 6.6 | 7.9 |
| ref | 7 | 19 | 20 | this work |

Table 4: Observed and Calculated Structural Parameters of Fe(II) Hexammine Complexes

| param | cryst structure | molecular mechanics | | |
|---|-----------------|---------------------|-----------------|-----------------|
| Low-Spin Fe(tacn) ₂ Cl ₂ ·4H ₂ O ^a | | | | |
| Fe ^{II} –N (Å) | 2.03 | 2.041 | | |
| ϕ^b (deg) | 59 | 59 | | |
| [Fe(<i>trans</i> -diammac)](PF ₆) ₂ | | | | |
| low spin | | $\delta\delta$ | $\delta\lambda$ | $\lambda\delta$ |
| Fe ^{II} –N _{eq} (Å) | 2.007 | 2.019 | 2.050 | 1.997 |
| Fe ^{II} –N _{ax} (Å) | 2.030 | 2.030 | 2.042 | 2.021 |
| θ^c (deg) | 11.5 | 8.1 | 16.9 | 2.7 |
| ΔH_{strain} (kJ mol ⁻¹) | | 82.19 | 96.47 | 87.42 |
| high spin | | | | hs |
| Fe ^{II} –N _{eq} (Å) | | 2.142 | 2.175 | 2.117 |
| Fe ^{II} –N _{ax} (Å) | | 2.189 | 2.206 | 2.178 |
| θ (deg) | | | | |
| ΔH_{strain} (kJ mol ⁻¹) | | 88.99 | 82.32 | 110.12 |
| High-Spin [Fe((NH ₃) ₂ sar)](NO ₃) ₄ ·H ₂ O ^{d,e} | | | | |
| Fe ^{II} –N (Å) | 2.21 | 2.195 | | |
| ϕ (deg) | 28.6 | 28.75 | | |

^a See ref 2. ^b Trigonal twist-angle. ^c Tilt angle. ^d C₃le₃ conformer. ^e See ref 1.

compounds of *trans*-diammac (~0.04 and ~0.06 Å, respectively) are as expected, on the basis of the general trends in metal–amine bond distances of first row transition metal compounds and the rigidity of the ligand; i.e., *trans*-diammac is enforcing extremely short metal–donor distances. This is responsible for the high ligand fields and the low reduction potentials observed in the corresponding transition metal compounds.²⁰ The expected^{5,6} and observed⁸ conformation of [Co(*trans*-diammac)]³⁺ is $\lambda\delta$, and that of the zinc(II)¹⁹ and iron(III)⁷ compounds is, as predicted, the same as for iron(II), i.e., $\delta\delta$.

Force field calculations (MM) were used for a conformational analysis of [Fe(*trans*-diammac)]²⁺ in high- and low-spin electronic configuration. For the low-spin compound the force field used leads to excellent agreement between observed and computed structures, with maximum Fe–N deviations of 0.01 Å. These results are presented in Table 4, which also includes the structural predictions (and observed parameters) for high-spin [Fe((NH₃)₂sar)]⁴⁺ and for low-spin [Fe(tacn)₂]²⁺. It emerges that (i) *trans*-diammac enforces the shortest bonds in the series and that (ii) with *trans*-diammac the order of bond distances is $\lambda\delta < \delta\delta < \delta\lambda$. It also appears that the strain energy of the high-spin $\delta\lambda$ conformer is identical to that of the low-spin $\delta\delta$ conformer.

For low-spin iron(II) the $\delta\delta$ conformer is most stable, and for the high-spin electronic configuration the $\lambda\delta$ geometry is

more stable, suggesting that a spin change would involve a conformational rearrangement. The activation energy of such a chelate ring inversion has been determined experimentally²¹ and by force field calculations^{6,22,23} to be approximately 20–25 kJ mol⁻¹. Variable-temperature magnetic measurements and UV–vis–NIR and ¹H NMR spectroscopy of [Fe(*trans*-diammac)]²⁺ indicate that, up to 373 K (solid-state and aqueous solution), there is no contribution of the high-spin electronic configuration, indicating that the difference in electronic energy between the two states is at least 200 kJ mol⁻¹. From the calculated strain energies one might assume that enforcing a $\delta\lambda$ conformation might help to stabilize the high-spin configuration, and this would be possible by a substitution of the five-membered chelate rings of the macrocycle. Relevant ligands, based on cyclohexane-1,2-diamine, have been reported but the separation into the pure isomers is a tedious and low-yielding procedure.²⁴ However, the stabilization of the high-spin isomer via steric effects would only result in spin crossover behavior if the electronic energy terms did not favor a particular ground state. With the large ligand field exerted by *trans*-diammac the stabilization of a high-spin state based on steric effects is extremely improbable.

The electronic spectrum of [Fe(*trans*-diammac)]²⁺ is consistent with a low-spin electronic configuration. There are two d–d transitions at 584 nm (17 120 cm⁻¹, $\epsilon = 100$ L mol⁻¹ cm⁻¹) and 405 nm (24 690 cm⁻¹, $\epsilon = 140$ L mol⁻¹ cm⁻¹), assigned to ¹A_{1g} → ¹T_{1g} and ¹A_{1g} → ¹T_{2g} (in *O_h*), respectively. Variable-temperature measurements (up to 373 K) indicate that there is no contribution of a high-spin configuration; i.e., the intensity of the two observed transitions is independent of the temperature. The comparably high molar extinction coefficients in L mol⁻¹ cm⁻¹ (100, 140 vs 6, 17 for [Fe(tacn)₂]²⁺ and 14 (¹A_{1g} → ¹T_{1g}) for [Fe((NH₃)₂sar)]²⁺) are expected for the distortion from octahedral geometry, observed in the crystal structure, and support the interpretation that the solution structure is similar (see Table 4). A simple ligand field analysis indicates that, among other low-spin iron(II) compounds, [Fe(*trans*-diammac)]²⁺ has, as expected, an extremely large value for *Dq* (1785 cm⁻¹ vs 1744 and 1674 cm⁻¹ for [Fe((NH₃)₂sar)]²⁺ and [Fe(tacn)₂]²⁺, respectively). The low value for the interelectronic repulsion parameter B of 567 cm⁻¹ (54% of the free ion value; the parameters for [Fe((NH₃)₂sar)]²⁺ and [Fe(tacn)₂]²⁺ are 659 cm⁻¹ (62%) and 753 cm⁻¹ (71%), respectively) indicates that *trans*-diammac is a strong σ donor, and this is in agreement with the coordination chemistry and ligand field spectroscopy of this ligand with other first row transition metal ions.^{5,7,8}

The combination of force field calculations with angular overlap model calculations (MM-AOM), i.e., the computation of electronic properties (e.g. d–d transitions) based on optimized structures, using transferable parameter sets for the structural and electronic calculations, has been used to predict and interpret the ligand field properties of transition metal compounds.^{6,7,20,25} The transferability of the parameters, in particular that of the electronic parameters, is problematic (we note specifically the differences in interelectronic repulsion emerging from the simple ligand field analysis of the low-spin iron(II) compounds

- (19) Bernhardt, P. V.; Lawrance, G. A.; Maeder, M.; Rossignoli, M.; Hambley, T. W. *J. Chem. Soc., Dalton Trans.* **1991**, 1167.
 (20) Comba, P.; Sickmüller, A. F. *Inorg. Chem.* **1997**, *30*, 4500.

- (21) Kuroda, Y.; Tanaka, N.; Goto, M.; Sakai, T. *Inorg. Chem.* **1989**, *28*, 997.
 (22) Hambley, T. W. *J. Comput. Chem.* **1987**, *8*, 651.
 (23) Bernhardt, P. V. *Inorg. Chem.* **1993**, *32*, 2804.
 (24) Bernhardt, P. V.; Hambley, T. W.; Lawrance, G. A.; Molloy, K. J. *Aust. J. Chem.* **1994**, *47*, 1171.
 (25) (a) Comba, P.; Hambley, T. W.; Hitchman, M. A.; Strateimer, H. *Inorg. Chem.* **1995**, *34*, 3903. (b) Comba, P.; Hilfenhaus, P.; Nuber, B. *Helv. Chim. Acta* **1997**, *80*, 1831. (c) Comba, P.; Sickmüller, A. F. *Angew. Chem., Int. Ed. Engl.* **1997**, *36*, 2006.

Table 5. Calculated (MM-AOM) and Observed Electronic Transitions (cm^{-1}) of Low-Spin Iron(II) Hexamine Complexes

| type | transition | | ref |
|--|---|--------|-----------|
| | [Fe(<i>trans</i> -diammac)] ²⁺ | | |
| $\delta\delta$ | 16 752 | 24 807 | |
| MM-AOM | 17 038 | 25 812 | |
| | 18 397 | 27 059 | |
| $\delta\lambda$ | 14 642 | 22 325 | |
| MM-AOM | 15 300 | 23 001 | |
| | 16 408 | 23 844 | |
| $\lambda\delta$ | 18 364 | 26 569 | |
| MM-AOM | 18 374 | 28 009 | |
| | 19 889 | 28 091 | |
| obsd ($\delta\delta$) | 17 123 | 24 691 | this work |
| | [Fe(tacn) ₂] ²⁺ | | |
| MM-AOM | 16 273 | 23 723 | |
| | 16 728 | 25 365 | |
| | 16 854 | 25 709 | |
| obsd | 16 639 | 25 840 | 2 |
| | [Fe((NH ₂) ₂ sar)] ²⁺ | | |
| MM-AOM | 15 944 | 23 944 | |
| | 16 393 | 24 581 | |
| | 16 842 | 25 650 | |
| obsd | 16 949 | 25 381 | 1 |
| obsd for [Fe((NH ₃) ₂ sar)] ⁴⁺ | 17 007 | 24 691 | 1 |

described above). However, extensive tests of the MM-AOM method^{6,7,20,25} indicate that, in general, results of reasonable accuracy may be expected. In particular, this has been shown for transition metal hexamines, involving, among others, *trans*-

diammac and its low-spin iron(III) and cobalt(III) compounds. The observed and computed d–d transition energies of low-spin [Fe(*trans*-diammac)]²⁺ and the corresponding tacn and sar compounds confirm this observation (Table 5; see Experimental for the parametrization used).

The $\delta\delta$ and $\lambda\delta$ isomers have similar strain energies (Table 4). Thus, both might be present in solution and contribute to the electronic spectrum. The comparison of computed and observed d–d transitions suggests that only the former, slightly more stable and experimentally observed species is present in appreciable concentration. The latter has significantly shorter Fe–N bonds and also a less distorted angular geometry ($\theta = 11.5^\circ$ (7.9° vs 2.7° (calculated values); see Table 4). Both these effects lead to a higher ligand field, and the computed differences are over 1000 cm^{-1} (approximately 40 nm for the low-energy transition).

Acknowledgment. Generous financial support by the German Science Foundation (DFG) and the Volkswagen-Stiftung is gratefully acknowledged. We are grateful to Dr. Gabor Laurenczy (University of Lausanne) for his help with some of the spectroscopic measurements.

Supporting Information Available: Four X-ray crystallographic files, in CIF format, are available. Access information is given on any current masthead page.

IC971552U